

Title	Atomistic study of GaN surface grown on Si(111)
Author(s)	Wang, Z. T.; Yamada-Takamura, Y.; Fujikawa, Y.; Sakurai, T.; Xue, Q. K.
Citation	Applied Physics Letters, 87(3): 032110-1-032110-3
Issue Date	2005-07-18
Type	Journal Article
Text version	publisher
URL	http://hdl.handle.net/10119/4527
Rights	Copyright 2005 American Institute of Physics. This article may be downloaded for personal use only. Any other use requires prior permission of the author and the American Institute of Physics. The following article appeared in Z. T. Wang, Y. Yamada-Takamura, Y. Fujikawa, T. Sakurai, and Q. K. Xue, Applied Physics Letters, 87(3), 032110 (2005) and may be found at http://link.aip.org/link/?APPLAB/87/032110/1
Description	

Atomistic study of GaN surface grown on Si(111)

Z. T. Wang

Institute for Materials Research, Tohoku University, Sendai 980-8577, Japan and Institute of Physics, Chinese Academy of Sciences, Beijing 100080, China

Y. Yamada-Takamura, Y. Fujikawa, and T. Sakurai

Institute for Materials Research, Tohoku University, Sendai 980-8577, Japan

Q. K. Xue

Institute of Physics, Chinese Academy of Sciences, Beijing 100080, China

(Received 18 March 2005; accepted 7 June 2005; published online 15 July 2005)

GaN is directly grown on Si(111) by radio-frequency plasma-assisted molecular-beam epitaxy, and the surface is studied using *in situ* reflection high-energy electron diffraction (RHEED) and scanning tunneling microscopy (STM). By optimizing the growth condition, well-defined surface reconstructions are observed in atomically-resolved STM images after the additional Ga deposition, indicating the uniform N-polarity of the grown film. We show that N-rich condition in the initial GaN growth and slightly Ga-rich condition in the subsequent growth are critical in order to achieve monopolar uniform GaN films. © 2005 American Institute of Physics. [DOI: 10.1063/1.2000332]

Gallium nitride growth has been extensively studied due to the applications of GaN-based materials as short-wavelength light emitting diodes and laser diodes. Various substrates, such as *c*-plane sapphire,^{1,2} 6H-SiC(0001),³ GaAs(111),⁴ and Si(111),^{2,5} have been used for wurtzite GaN growth due to the lack of large size GaN single-crystal. Among these substrates, Si is considered the most attractive because of its mature electronic industry and availability of high quality, low cost, and large diameter wafers. However, it is difficult to grow high quality GaN directly on the Si substrate because of the large lattice mismatch and the difference in thermal expansion coefficient between GaN and Si. Therefore, buffer layers, such as AlN,^{6,7} SiC,^{5,8} GaAs,⁹ ZrB₂,¹⁰ and thin silicon nitride,¹¹ have been developed to overcome the problems. The AlN layer is by far the most widely employed, but silicon nitride layer formation by substrate nitridation is the simplest solution since it only requires exposure of a substrate to a nitrogen source prior to GaN growth. The wurtzite structure of GaN has freedom in its polarity, which in turn has direct influence on surface structure, growth process, and its quality.^{12,13} The polarity is largely influenced by the choice of the substrate and the buffer layer used for the initial film nucleation.^{3,12} In the case of a nonpolar substrate like Si, it is especially important to control the nucleation stage in order to accomplish monopolar film with atomically-smooth surface.

In this letter, we report on our RHEED and STM study of GaN surfaces grown directly on Si(111) using radio-frequency (rf) plasma-assisted molecular-beam epitaxy (PAMBE). The initial nucleation and the subsequent growth stages of GaN are studied in detail to determine their influence on the surface morphology.

GaN is grown in an ultrahigh vacuum (UHV) MBE-SPM system, which consists of three UHV chambers (SPM, XPS, and MBE) with base pressures better than 1.0×10^{-8} Pa and an additional high vacuum load-lock chamber. The MBE chamber is equipped with a *K*-cell for gallium and an rf plasma source for activated nitrogen, and the growth can be monitored *in situ* and in real time by RHEED. The *n*-type P-doped Si(111) substrate is ultrasonically cleaned by

acetone, and loaded into the MBE chamber via the load-lock chamber. The Si substrate is heated by direct current and the temperature is measured by an infrared pyrometer. After degassing for several hours at 600 °C and then heated up to 1250 °C for 3–5 min, the Si substrate shows the 7×7 reconstruction in both RHEED and STM. In our experiments, the Si substrate is nitridated by nitrogen plasma (rf power: 300 W; N₂ pressure: 2×10^{-3} Pa) at a substrate temperature of 700 °C for 3 min to form a silicon nitride layer prior to the growth. After that, GaN is grown under varying nucleation and growth conditions. GaN is initially nucleated and grown at substrate temperature of 700 °C for 10 min under the same nitrogen plasma condition as the substrate nitridation condition. Three different Ga *K*-cell temperatures are used to grow nucleation layer, 980 °C [beam equivalent pressure (BEP): 1.3×10^{-4} Pa], 950 °C (BEP: 0.8×10^{-4} Pa), and 900 °C (BEP: 0.4×10^{-4} Pa), which correspond to conditions A, B, and C, respectively. Following the nucleation layer growth, the substrate temperature is increased to 730–800 °C and the Ga *K*-cell temperature to 1020–1090 °C (BEP: 2.2 – 5.5×10^{-4} Pa). Nitrogen plasma condition is set at rf power of 300 W and N₂ pressure of 3×10^{-3} Pa. For another set of samples, GaN is nucleated and grown at a fixed substrate temperature of 750 °C, and two different Ga *K*-cell temperatures are used for the nucleation layer growth: 980 °C (BEP: 1.3×10^{-4} Pa) and 1050 °C (BEP: 3.5×10^{-4} Pa), which correspond to conditions D and E, respectively. The nitrogen plasma condition is set similar to the final growth conditions of A, B, and C. After 10–20 min of nucleation layer growth, the *K*-cell temperature for growth condition D is increased to 1050 °C. The total growth time for all the samples is in the range of 2–4 h. RHEED and STM are used to identify the morphology and reconstructions of the GaN surface.

After the nitridation of the Si(111) substrate, the RHEED pattern shows no clear spots or streaks indicating the amorphous nature of the nitride layer. At the nucleation stage of GaN on the nitride layer, RHEED shows a spotty pattern, indicating three-dimensional (3D) growth. From the RHEED pattern, GaN is determined to be wurtzitic and grows with

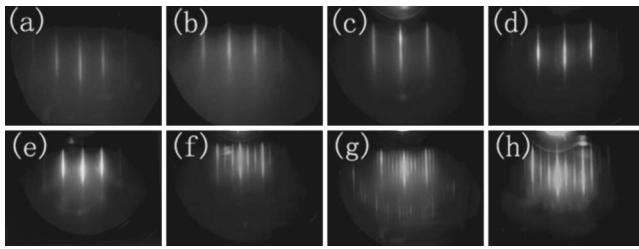


FIG. 1. RHEED patterns of GaN films deposited on Si(111), observed with an electron beam parallel to GaN $\langle\bar{1}\bar{1}20\rangle$, displaying GaN{0001}- (a) 1×1 and (b) faint 3×3 patterns for the samples grown under condition A, (c) 1×1 and (d) 3×3 patterns for the samples grown under conditions B and E, and (e) 1×1 , (f) 3×3 , (g) 6×6 , and (h) $c(6\times 12)$ patterns for the samples grown under conditions C and D.

the following epitaxial relationship between the Si(111) substrate: GaN $\langle 0001\rangle\parallel\text{Si}\langle 111\rangle$ and GaN $\langle\bar{1}\bar{1}20\rangle\parallel\text{Si}\langle 1\bar{1}0\rangle$, similar to the result in Ref. 11. Due to the surfactant effect of excess Ga on the surface,^{13,14} the growth mode of some samples changes to two-dimensional (2D) growth after certain deposition time, which is observed in change from spotty to streaky RHEED pattern. We call this growth condition Ga-rich, and the growth condition with less Ga flux N-rich that gives spotty RHEED pattern even after growth for longer time.¹⁵ At the nucleation layer growth stage, conditions A, B, and E are Ga-rich since 2D growth mode is achieved after short time GaN growth. As no streaky RHEED pattern is observed at the nucleation stage for the samples grown under conditions C and D, these conditions are N-rich. After the nucleation layer growth, all of the samples are grown in slightly Ga-rich condition that yields streaky 1×1 RHEED pattern during and after growth as shown in Figs. 1(a), 1(c), and 1(e).

The difference due to the growth conditions A to E, can be observed clearly when we deposit Ga on the GaN surface at room temperature to obtain surface reconstructions. For the samples grown under condition A, no additional reconstruction is achieved by changing Ga coverage on the 1×1 surface besides faint 3×3 appearing occasionally [Fig. 1(b)]. For the samples grown under conditions B and E, 3×3 and occasionally 6×6 RHEED patterns are observed, but no $c(6\times 12)$ is observed [Fig. 1(d)]. On the other hand, for those grown under conditions C and D, the RHEED patterns show clear and high intensity 3×3 , 6×6 , and $c(6\times 12)$ patterns [Figs. 1(f)–1(h)] depending on the amount of Ga deposited on the 1×1 surface. These reconstructions confirm that these GaN films have N-polarity.¹⁶ When we heat up these films above the critical temperature, the reconstruction phases reversibly transfer to 1×1 due to Ga diffusion as previously reported.¹⁷

Using STM, atomic resolution images for the 3×3 , 6×6 , and $c(6\times 12)$ reconstructions shown in Fig. 2 are obtained for the samples grown under conditions C and D. The images are similar to those reported by Smith *et al.*¹⁶ Figure 2(a) shows an image in the size of 200 nm square covered with $c(6\times 12)$ reconstruction. The step height is about 0.26 nm, half the lattice constant along the c -axis of wurtzite GaN unit cell, corresponding to a bilayer step. These STM images confirm that the surface is covered with N-polar related reconstructions and the terrace size is in the range of 50–250 nm. Increasing the amount of Ga on this surface does not induce further reconstruction or fluid surface, and

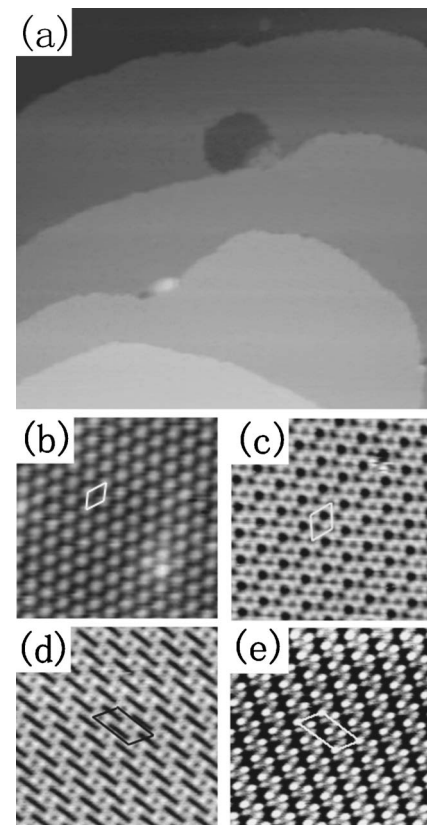


FIG. 2. STM images of the samples grown under conditions C and D. (a) Scan size $200\times 200\text{ nm}^2$ showing $c(6\times 12)$ reconstruction, (b) $10\times 10\text{ nm}^2$ showing 3×3 reconstruction, (c) $15\times 15\text{ nm}^2$ showing 6×6 reconstruction, and (d) and (e) $15\times 15\text{ nm}^2$ showing $c(6\times 12)$ reconstruction. Sample bias voltages are -0.45 V , -0.25 V , $+0.70\text{ V}$, -3.8 V , and $+2.1\text{ V}$, respectively.

only the formation of clusters is observed in STM images. For the samples grown under condition A, the surface is very rough, and no ordered phase is observed by STM. Although STM images for the samples grown under conditions B and E are also rough, small size $c(6\times 12)$ reconstructed domains are observed frequently at relatively flat area indicated by an arrow [Fig. 3(a)]. Occasionally, very flat areas without any atomic feature coexisting with the $c(6\times 12)$ reconstructed areas can be seen in the STM images [Fig. 3(b), regions II, IV, V] when the sample is grown under condition B. These flat, featureless areas are likely due to Ga-fluid over the Ga-polar crystal.^{18,19} “Brighter feature” at the edge of the fluid island reported in Ref. 19 is also seen. The observed boundary planes between the $c(6\times 12)$ reconstructed areas and featureless areas are $\{1\bar{1}00\}$, which is a typical inversion domain boundary.²⁰ The Ga-rich condition is known to make growth rates of Ga-polar and N-polar crystals similar.²¹ All these facts suggest that this surface is mixed in polarity with N-polar regions I and III and Ga-polar regions II, IV, and V.

Since the substrate nitridation condition and the final GaN growth condition are similar for all the samples, the nucleation layer growth condition must be the critical process to determine the formation of surface reconstruction. The samples grown under conditions C and D, which show clear atom-resolved reconstructions, are initially grown under the N-rich condition, while those grown under conditions A, B, and E, which results in poorly reconstructed surface, are initially grown under Ga-rich conditions. Our optical mi-

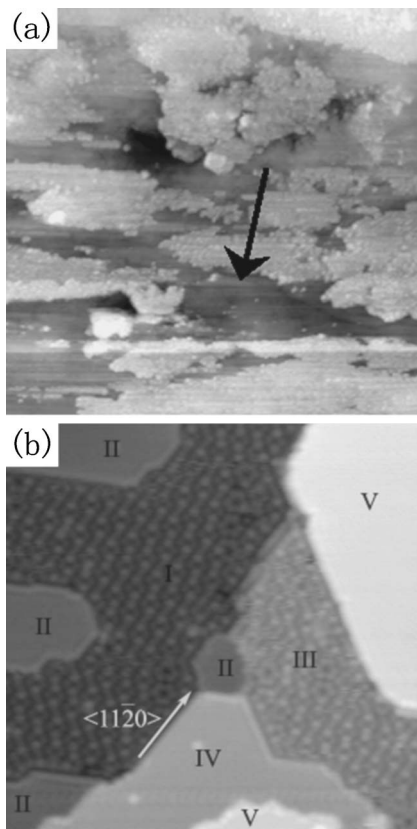


FIG. 3. Typical STM images observed on the samples grown (a) under conditions B and E, and (b) under condition B. (a) Scan size $720 \times 720 \text{ nm}^2$ showing the rough surface with relatively flat area indicated by an arrow, where small $c(6 \times 12)$ reconstructed domains are observed frequently, and (b) $30 \times 30 \text{ nm}^2$ showing the fluid islands coexisting with the $c(6 \times 12)$ reconstructed areas. Sample bias voltages are $+1.5 \text{ V}$ and -0.4 V , respectively.

roscope observations (not shown) indicate that the Ga flux in the nucleation layer growth stage of condition A is so high to form droplets on the surfaces. Ga droplets are known to dissolve Si above 500°C resulting in a rough surface as observed by STM. For the samples grown under conditions B and E, no droplets are formed on the surfaces, indicating the proper composition of the deposit. Therefore, it appears that the poor quality of these surfaces resulting in diffuse RHEED patterns and rough STM images is caused by the mixed-polar nucleation and growth as observed in Fig. 3(b).

The N-rich condition in the nucleation layer growth stage of GaN appears to be critical for accomplishing atomically-smooth monopolar GaN surface with well-defined reconstructions. In PAMBE, N-rich growth condition is known to increase the growth rate of the Ga-polar crystal compared to the N-polar crystal²¹ and has been used to allow

Ga-polar crystal to outgrow N-polar crystal.²² Therefore, the N-rich condition in our case should be playing an important role on nucleating only the N-polar GaN on the Si substrate similar to the case of inversion domainless GaN film grown on *c*-plane sapphire using ECR-MBE under relatively N-rich condition.²³

In summary, epitaxial and monopolar GaN is successfully grown directly on Si(111) by PAMBE upon nitridation of the substrate and selective N-polar nucleation under N-rich condition. The GaN surface shows well-defined GaN(000 $\bar{1}$)- 3×3 , 6×6 , and $c(6 \times 12)$ reconstructions observed by RHEED and STM, proving the uniform polarity.

¹S. Nakamura, Jpn. J. Appl. Phys., Part 1 **30**, L1705 (1991).

²T. D. Moustakas, T. Lei, and R. J. Molnar, Physica B **185**, 36 (1993).

³T. Sasaki and T. Matsuoka, J. Appl. Phys. **64**, 4531 (1988).

⁴H. Okumura, S. Misawa, and S. Yoshida, Appl. Phys. Lett. **59**, 1058 (1991).

⁵T. Takeuchi, H. Amano, K. Hiramatsu, N. Sawaki, and I. Akasaki, J. Cryst. Growth **115**, 634 (1991).

⁶A. Watanabe, T. Takeuchi, K. Hirose, H. Amano, K. Hiramatsu, and I. Akasaki, J. Cryst. Growth **128**, 391 (1993).

⁷A. M. Sanchez, P. Ruterana, S. I. Molina, F. J. Pacheco, and R. Garcia, Phys. Status Solidi B **234**, 935 (2002).

⁸D. Wang, Y. Hiroyama, M. Tamura, M. Ichikawa, and S. Yoshida, Appl. Phys. Lett. **76**, 1683 (2000).

⁹J. W. Yang, C. J. Sun, Q. Chen, M. Z. Anwar, M. Asif Khan, S. A. Nikishin, G. A. Seryogin, A. V. Osinsky, L. Chernyak, H. Temkin, C. Hu, and S. Mahajan, Appl. Phys. Lett. **69**, 3566 (1996).

¹⁰J. Tolle, R. Roucka, I. S. T. Tsong, C. Ritter, P. A. Crozier, A. V. G. Chizmeshya, and J. Kouvetakis, Appl. Phys. Lett. **82**, 2398 (2003).

¹¹Y. Nakada, I. Aksenov, and H. Okumura, Appl. Phys. Lett. **73**, 827 (1998).

¹²E. S. Hellman, MRS Internet J. Nitride Semicond. Res. **3**, 11 (1998).

¹³G. Mula, C. Adelman, S. Moehl, J. Oullier, and B. Daudin, Phys. Rev. B **64**, 195406 (2001); N. Gogneau, E. Sarigiannidou, E. Monroy, S. Monroy, H. Mank, and B. Daudin, Appl. Phys. Lett. **85**, 1421 (2004).

¹⁴E. Monroy, E. Sarigiannidou, F. Fossard, N. Gogneau, E. Bellet-Amalric, J.-L. Rouvière, S. Monroy, H. Mank, and B. Daudin, Appl. Phys. Lett. **84**, 3684 (2004).

¹⁵E. J. Tarsa, B. Heying, X. H. Wu, P. Fini, S. P. DenBaars, and J. S. Speck, J. Appl. Phys. **82**, 5472 (1997).

¹⁶A. R. Smith, R. M. Feenstra, D. W. Greve, J. Neugebauer, and J. E. Northrup, Phys. Rev. Lett. **79**, 3934 (1997); Appl. Phys. A: Mater. Sci. Process. **A66**, S947 (1998).

¹⁷A. R. Smith, R. M. Feenstra, D. W. Greve, M.-S. Shin, M. Skowronski, J. Neugebauer, and J. E. Northrup, Appl. Phys. Lett. **72**, 2114 (1998).

¹⁸A. R. Smith, R. M. Feenstra, D. W. Greve, M. S. Shin, M. Skowronski, J. Neugebauer, and J. E. Northrup, J. Vac. Sci. Technol. B **16**, 2242 (1998).

¹⁹Q. Z. Xue, Q. K. Xue, R. Z. Bakhtizin, Y. Hasegawa, I. S. T. Tsong, T. Sakurai, and T. Ohno, Phys. Rev. B **59**, 12604 (1999).

²⁰L. T. Romano, J. E. Northrup, and M. A. O'Keefe, Appl. Phys. Lett. **69**, 2394 (1996).

²¹L. T. Romano and T. H. Myers, Appl. Phys. Lett. **71**, 3486 (1997).

²²E. C. Piquette, P. M. Bridger, Z. Z. Bandic, and T. C. McGill, J. Vac. Sci. Technol. B **17**, 1241 (1999).

²³L. T. Romano, B. S. Krusor, R. Singh, and T. D. Moustakas, J. Electron. Mater. **26**, 285 (1997).